RESEARCH ARTICLE

Two ResNet Mini Architectures for Aircraft Wake Vortex Identification

SIYUAN DUAN[1,2], WEIJUN PAN[2], YUANFEI LENG[2], AND XIAOLEI ZHANG[3]

[1]Tianfu Engineering-Oriented Numerical Simulation and Software Innovation Center, Sichuan University, Chengdu 610207, China
[2]College of Air Traffic Management, Civil Aviation Flight University of China, Guanghan 618307, China
[3]Department of Medical Imaging, Second Clinical Institute, Shantou University Medical College, Shantou 515041, China

Corresponding authors: Weijun Pan (wjpan@cafuc.edu.cn) and Xiaolei Zhang (bmezhang@vip.163.com)

ABSTRACT The identification of aircraft wake vortex is an essential issue in the operation of airspace utilization ratio. In particular, accurately identifying wake vortex in fine classification is helpful to guide separation standards under realistic airport conditions that consist of various complex operation scenarios. To stress this issue and improve the efficiency at the same time, we developed two mini architectures with each network of 10 layers by modifying deep residual neural network (ResNet) and describe the results of a study to evaluate the performances for identifying wake vortex in fine classification. For this purpose, we built the wake vortex dataset measured with pulsed Doppler LiDAR at Chengdu Shuangliu International Airport from Aug 16, 2018, to Oct 10, 2018. To support wake vortex identification in fine classification, the classification indices that consider the background wind speeds, wake vortex evaluation and aircraft types were included in the learning and identification tasks. We compared the performance of the two ResNet mini architectures with other lightweight networks by using wake vortex dataset. The experimental results demonstrate that the developed two ResNet mini architectures contribute to competitive wake identification modeling in terms of accuracy and parameter number.

INDEX TERMS Wake vortex identification, LiDAR, lightweight network, ResNet.

I. INTRODUCTION

The turbulence generated by aircraft wave vortex during the landing and take-off phases of the flight presents a potential hazard to the trailing aircraft, this limits airport capacity [1], [2], [3]. On the other hand, due to the low flight altitude of the aircraft and the limited response time of the pilot [4], the aircraft wake vortex of near surface has an important influence on flight safety [5]. From 1983 to 2000, the National Transportation Safety Board recorded more than 130 flight accidents caused by wake turbulence, accounting for 1/3 of the total number of air accidents in the United States during the period [6], [7]. The International Civil Aviation Organization (ICAO) has stipulated aircraft wake separation standards to assure air traffic safety [1], [8]. However, current ICAO wake separation rules are relatively conservative and have become an important factor limiting the development of the current civil aviation industry [8], [9]. To cope with the rapid growth of flight capacity, it is essential to bring the increased insight into aircraft wave vortex analysis.

There exist two important methods to study the behavior of aircraft wake, i.e., computational fluid dynamics (CFD) and flow field measurement [10]. The main advantage of CFD is that it supports the consistent analysis of wake vortex behavior under various environmental conditions, but this technique cannot exhibit a significant impact on aircraft spacing to improve airport capacity [11]. Compared to CFD, the high precision and resolution of LiDAR make it capable of supporting the most effective field measurement [11]. Specifically, in clear air the LiDAR is the effective sensors, as the

The associate editor coordinating the review of this manuscript and approving it for publication was Emre Koyuncu.

echoes are mainly derived by the particles involved in the wake vortex [8]. In another two works [10], [12], we have briefly outlined the analyzed techniques for aircraft wake vortex.

In particular, the intensity data provided by the products of pulsed Doppler LiDAR can be used to mine information of wake vortex observed. However, signal uncertainty and eccentricity caused by sensor scanning patterns, background winds and a receiver's adjusted gain response usually exist in the data of wake vortex provided by pulsed Doppler LiDAR. So, the large number of lower quality materials makes it very hard for manual methods to reliably identify the informational parts in wake vortices, which is labor and time consumption. Moreover, these manual means require the intervention of experts in the process. In such situations, computational methods provide the program capabilities to identify aircraft wave vortex.

To perform accurate identification of wake vortices, a natural solution of the problem is to extract and enhance their weak features embedded in inhomogeneous backgrounds. Since the results of LiDAR products can be supported by information content that extends the pixel information, the strategies of deep leaning can provide good prospective tools. In this study, we conducted a deep learning based study to identify air wake vortex. In the process of deep learning technology into application, there are two key innovations:

• Fine classification for wake vortex identification. Some existing deep learning based methods [13], [14], [15] mainly focus on achieving better identification accuracy in binary classification, i.e., wake vortex and non wake vortex. However, fine classification in identifying wake vortex is an important criterion in the applications of guiding aircraft wake separation standards, which satisfies the various complex requirements of users. To better exploit the potential in separation standards under realistic airport conditions, classification indices that consist of the background wind speeds, wake vortex evaluation and aircraft types were included in the identification task.

• Use efficiency. To be effective, neural networks for wake identification tasks should be lightweight, in which the better spatial inductive biases allow networks to learn representations with fewer parameters. Towards this end, we developed two networks with each of 10 layers by modifying deep residual neural network (ResNet) [16], named as ResNet mini v1 and ResNet mini v2, to extract the features of considered materials and test them in wake vortices of various scene. Case studies indicate that the proposed two networks exhibit competitive results across different tasks that comprehensively consider background wind speeds, wake evaluation, three aircraft types and parameter number.

The remainder of the paper is organized as follows. Section II describes the data resource and its classification index. The proposed two identification models are introduced in Section III. Experiments and results are presented in Section IV, Section V is the conclusions and the limitations and future work are drawn in Section VI.
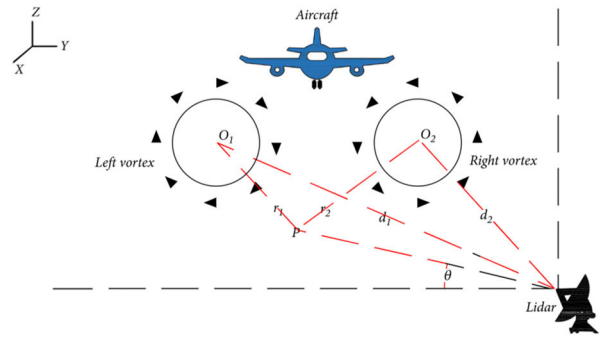

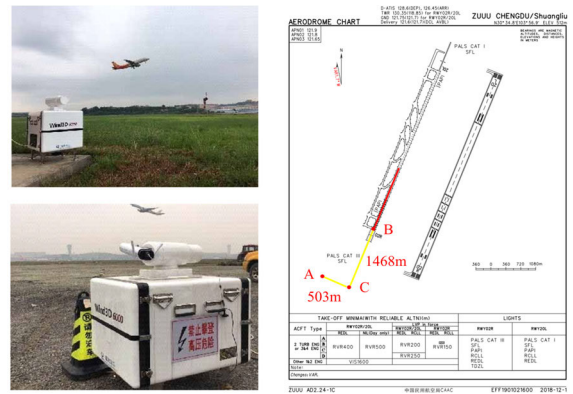**FIGURE 1.** RHI scans for wake vortex measurement.

FIGURE 2. Aircraft Wake Vortex Field Detection by wind3D 6000.

TABLE 1. The parameters of Wind3D 6000 and experimental configuration (RHI) for measuring aircraft wake vortex at the chengdu shuangliu internal airport from aug 16, 2018, to oct 10, 2018.

Category	Parameter	Value
Qualification Specification	Wavelength (um)	1.55
	Pulse repetition (kHz)	10
	Sampling rate (GHz)	1
	Data update rate (Hz)	4
	Pulse width (ns)	100-400
	Pulse energy (uJ)	150
	Measurement range (m)	45-6000
	Range resolution (m)	15-50
LiDAR parameters	Azimuth angle (°)	112
	Scanning rate (°/s)	1
	Elevation range(°)	0-10
	Elevation angle resolution (°)	0.2±0.03
	Detection radial range (m)	45-885
	Longitudinal resolution (m)	15
	Distance between point A and B (m)	503
	Distance between point B and C (m)	1468

II. DATA RESOURCES

A. DATA COLLECTION

In practice, we use rhi (range height indicator) scans [10], [12] to measure wake vortex, which provide a two-dimensional perspective of the turbulence. The measurements performed rhi scans indicated by the dashed lines are shown in **Fig. 1**. The rhi scans are used to calculate vertical

cross-section profiles of wake vortices over the whole scan area, allowing the position of the lidar (point a in the right of **Fig. 2**). The mode of the lidar used for the experiment is Wind3D 6000 (showed in the left of **Fig. 2**), which is manufactured by leica-lidar transient technology ltd. The parameters of wind3d 6000 and experimental configuration (rhi) are detailed in **Table 1**. In our work, we use Wind3D 6000 to measure aircraft wake vortex at the chengdu shuangliu internal airport from aug 16, 2018, to oct 10, 2018.

B. DATA VISUALIZATION AND PROCESSING

For a better observation of wake vortex, we transform the original material into intensity data. to set up the most direct and effective way of satisfying the model of deep learning, the wake data is visualized using a gray cloud image with linear mapping. **Fig. 3** shows an example of this operation on aircraft wake vortex of AIRBUS-A320.
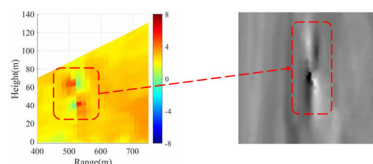

FIGURE 3. Transformation for aircraft wake vortex of Airbus-A320.

C. DATA AUGMENTATION AND ORGANIZATION

The primordial dataset is comprised of 3531 samples, which is divided into two parts. The first part contains 750 samples of existing aircraft wake vortex, the second part is that without aircraft wakes. To offer a richer and more balance dataset, we rotated 0 to 2 degrees, or panned left, right, up, and down on each sample for dataset extension. After that, we remove the impure data, and then we got a total of 15,000 samples. Among them, each category accounts for half. Besides, we changed all images from 336×288 to 100×100, to reduce the occupation of computer memory. **Fig. 4** is the operations for the dataset extension. And then, we divide the dataset into three parts, the training set, the validation set, and the test set, accounting for 60%, 20%, and 20% respectively.

FIGURE 4. Image augmentation for the intensity data of aircraft wake vortex.

D. SPECIFICALLY SPLIT THE TEST SET

1) BACKGROUND WIND FIELD

The visualization of aircraft wake vortex under background wind field with different speed is displayed in **Fig. 5**. From this figure, the cross wind provides additional turbulent kinetic energy input to the wake vortex, and the vorticity of the vortex core increases rapidly with greater axial velocity and rolling moment than that in the case of static wind. For wake vortex motion, encountering crosswind will accelerate

the wake vortex to be blown away from the route. For the strength dissipation of the wake vortex, the low-speed wind is not enough to destroy its morphological integrity when the wake vortex receives continuous cross wind disturbance, while the strong cross wind can adequately accelerate the separation and dissipation of the wake vortex core of the aircraft [18], [19]. Therefore, the identification of wake vortex in strong wind field is equally important to that in weak wind field. In this work, the wake vortex data under wind speed 4m/s and 1m/s are considered in the test models.
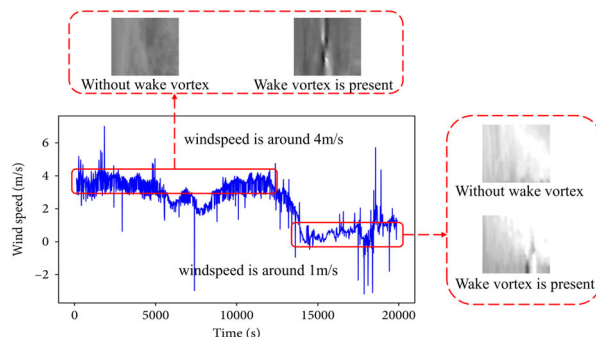

FIGURE 5. Average wind variation in background wind field.
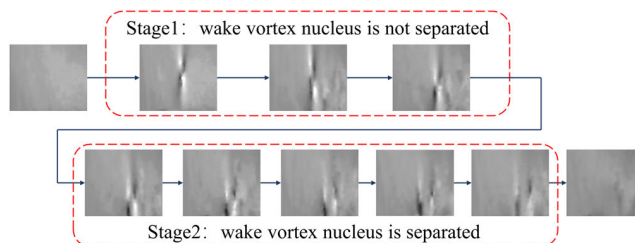

FIGURE 6. Evolution of aircraft wake vortex. According to whether the aircraft wake vortex cores are separated, we can roughly divide the wake cycle into two stages. The first stage is that the vortex nuclei is not separated, and the second stage is separated.

FIGURE 7. Visualization of wake vortex data in aircrafts of three types.

2) CYCLE STAGES OF WAKE VORTEX

Fig. 6 shows the entire cycle of the wake from generation to gradual dissipation. At the beginning of the aircraft wake, its radial velocity is very fast, and the positions of the two vortices are very close. Under the time evolution, the radial velocity of wake vortex gradually decreases to 0 due to the frictional force of the surrounding air, and the distance between two vortex nuclei gradually increases until dissipated. following this, we divided the wake cycle into two stages based on whether the aircraft wake vortex cores are separated in the test models.
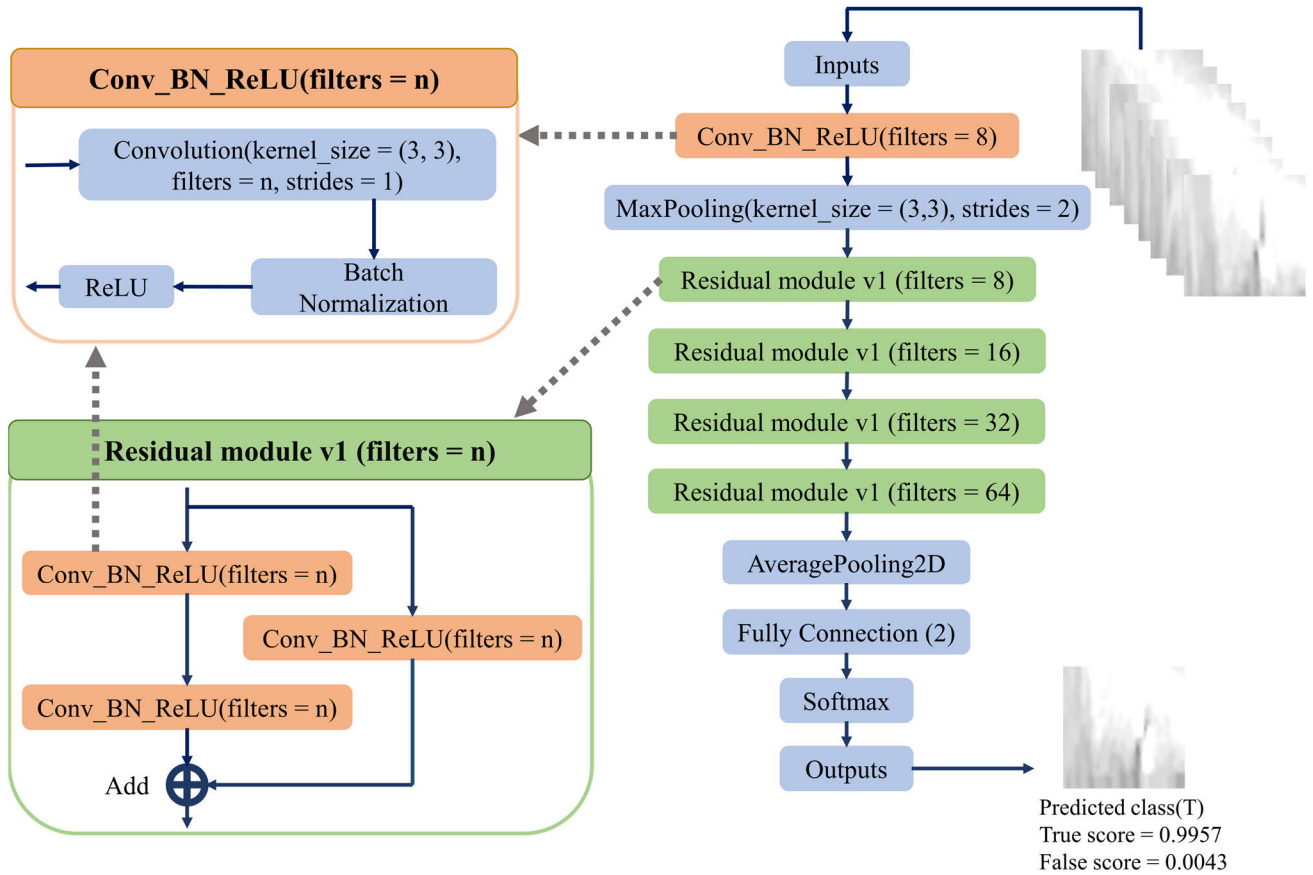
FIGURE 8. ResNet mini v1 Architecture.

TABLE 2. Test accuracy on different scenes and total parameters of models.

	ResNet mini v2	ResNet mini v1	CNN	LeNet-5	SqueezeNet v1	ShuffleNet v1 (group=1)
Cycle stage 1	**0.9500**	0.9250	0.8875	0.9375	0.9250	0.9375
Cycle stage 2	0.9375	0.9500	0.8750	**0.9625**	0.9375	0.9500
Background windspeed (around 1m/s)	0.9750	**0.9875**	0.9625	**0.9875**	**0.9875**	0.9500
Background windspeed (around 4m/s)	0.9125	0.9000	0.8125	**0.9250**	0.8875	0.9250
Light aircraft	0.9173	0.9202	0.8822	0.9120	**0.9268**	**0.9268**
Medium aircraft	**0.9587**	0.9493	0.9457	0.9420	0.9500	0.9304
Heavy aircraft	**0.9740**	0.9683	0.9613	0.9613	0.9613	0.9577
Overall	**0.9467**	0.9440	0.9253	0.9340	0.9433	0.9337
Total parameters	134,812	**80,010**	130,306	1,213,326	1,266,426	1,102,034

3) AIRCRAFT TYPES

Different types of aircraft with the corresponding wake flow strength are considered in the test models. **Fig. 7** provides the visualization of wake data in aircrafts of three types: light aircraft, medium aircraft and heavy aircraft.

III. RESNET MINI

In this section, we modified ResNet framework [16] to lead to the proposed ResNet mini v1 and ResNet mini v2. Each network is 10 layers deep, which can significantly reduce the network parameters while enhancing the performance.

The reason of selecting a mini version of ResNet is that we aim to reduce the risk of overfitting and make it manageable for hardware devices to execute, allowing time reduction and facilitated operation in the actual civil aviation equipment.

A. RESNET MINI V1

Fig. 8 depicts the architecture of ResNet mini v1. The ResNet mini v1 consists of a Block named Conv_BN_ReLU [20] followed by a max pooling layer, four Residual Modules, an average pooling layer, a fully connected layer, and a softmax at the end.
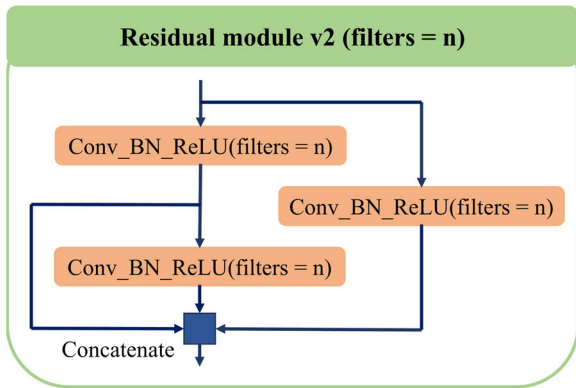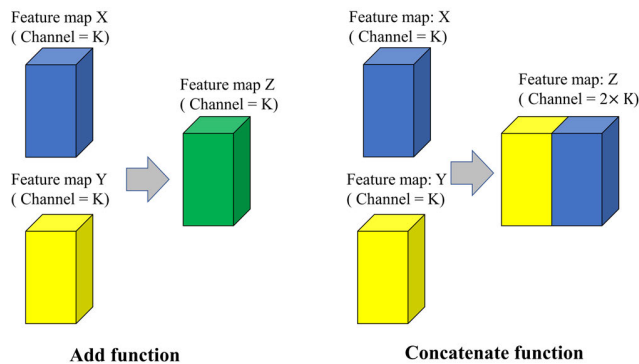
FIGURE 9. Structure of Residual module v2.

FIGURE 10. Add function and Concatenate function.

FIGURE 11. ResNet mini v2 Architecture.

In Cov_BN_ReLU block, Batch Normalization (BN) [21] is added between the convolution layer with kernel size 3-by-3, stride 1 and padding of 3 pixels, and max pooling layer with kernel size 3-by-3, stride 2 and padding of 1 pixel. It can greatly improve the speed of model training and accelerate the convergence speed.

Residual module consists of three Conv_BN_ReLU blocks as shown in the lower left corner of **Fig. 8**. The amounts of filters in the convolution layers of residual module also doubles as the network deepens. The last Residual module is connected to an average pooling and then a fully connected layer follows. There are two neurons in the fully connected layer for solving the binary problem. At the end of the network is a softmax function.

B. RESNET MINI V2

To incorporate more features from different layers and ensure their reusability, inspired by DenseNets [22], we improved Residual module v1 and designed a Residual module v2, as shown in **Fig. 9**.

In our Residual module v2, the characteristics of different layers are further integrated by adding a skip connection, which alleviates the disappearance of gradient and improves the back propagation of gradient, making the model easier to train. Compared with add function, the use of concatenation function can achieve feature connection on channels, thus it improves feature map capability of describing the image
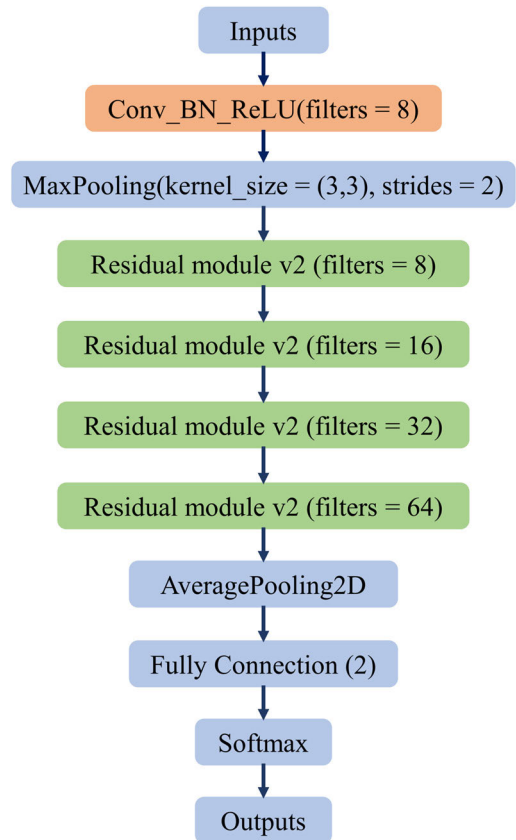
information (**Fig. 10**). Although the model parameters are slightly increased, it can improve the efficiency of feature reuse in the network.

For ResNet mini v1, by replacing Residual module with Residual module v2, we will get ResNet mini v2 framework (**Fig. 11**).

IV. RESULTS AND DISCUSSION

To identify wake vortices within our dataset, the ResNet mini based method is described as the flow chart of **Fig. 12**.

A. EXPERIMENTAL PLATFORM AND NETWORK PARAMETER SETTING

In our experiments, the workstation used in this study is a computer with 8G memory, Intel i7-8565U CPU, a 1.80G main operating frequency, and a GeForce MX150 (2GB) GPU.

The deep convolutional neural network is built on the tensorflow1.9 framework and is implemented using Python3.6. The number of batch size is 5, the number of epochs is 20. Optimizer is Adam [23], learning rate is 0.00001 with decay 0.00001/20. The Binary Cross-entropy is used as loss function.

B. EXPERIMENTAL RESULTS

For comparison analysis, four lightweight networks CNN [13], LeNet-5 [24], SqueezeNet v1 [25] and ShuffleNet
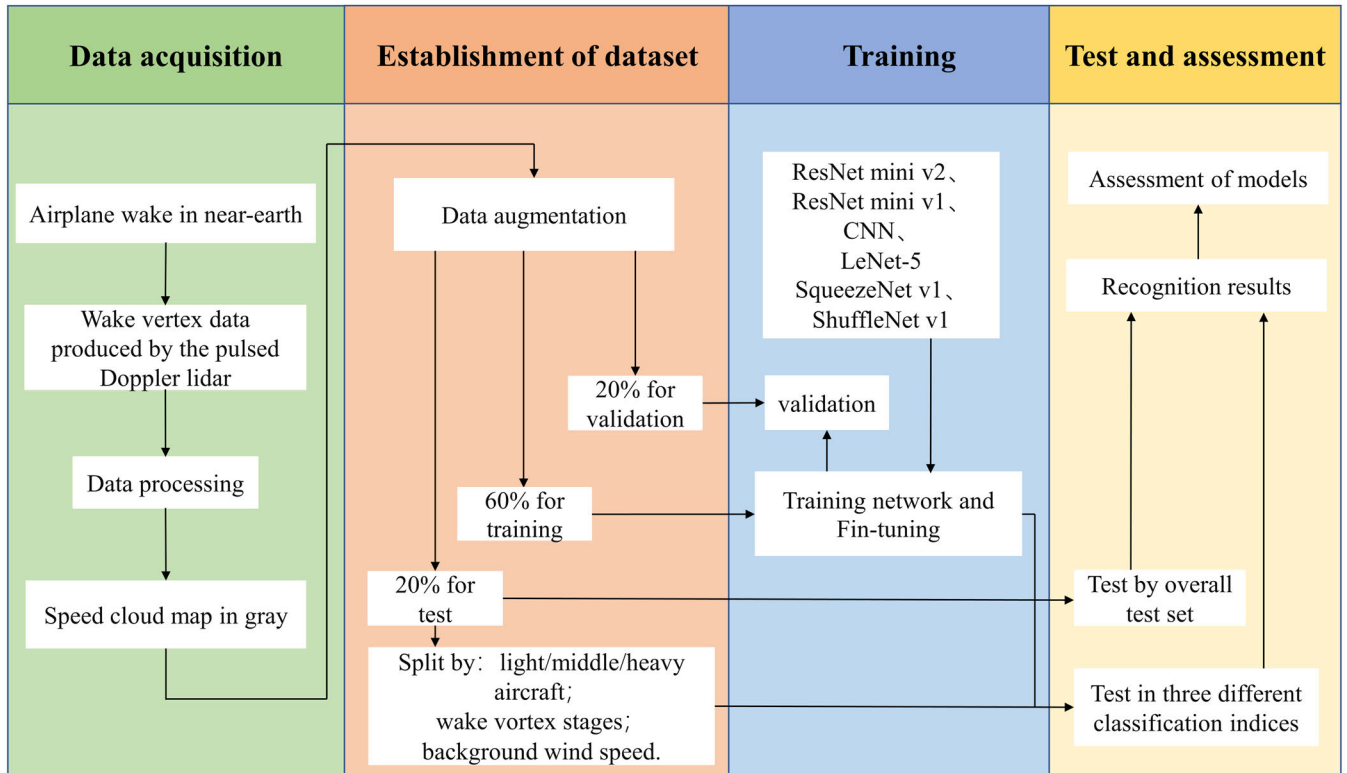
FIGURE 12. Flow chart of the ResNet mini wake identifying algorithm.

v1 [26], with each of parameter number close to ResNet mini architecture, are considered in experimental evaluation by using our wake vortex dataset. The parameter numbers of ResNet mini v1, ResNet mini v2, CNN, LeNet-5, SqueezeNet v1 and ShuffleNet v1 are 80,010, 134,812, 130,306, 1,213,326, 1,266,426 and 1,102,034 respectively when they are applied to wake vortex identification.

The loss and accuracy curves of models over epochs in training and validation for the wake vortex dataset are illustrated in **Fig. 13**. It is clear that the training accuracies obtained by ResNet mini v1 and ResNet mini v2 are closed to SqueezeNet v1 but much better than that of CNN. In validation accuracy, ResNet mini v1 and ResNet mini v2 present results close to those of LeNet-5, SqueezeNet v1 and ShuffleNet v1, while they exceed the performance of CNN. What's more, apparently, ResNet mini v1 has only 61.4%, 6.6%, 6.3% and 7.3% parameters of CNN, LeNet-5, SqueezeNet v1 and ShuffleNet v1 on the verification set. In addition, ResNet mini v2 exhibits only 11.1%, 10.6% and 12.2% parameters of LeNet-5, SqueezeNet v1 and ShuffleNet v1 for verification.

For quantitative comparison of identification methods on the wake vortex test set, the model's performances are evaluated by several measures: receiver operating characteristic (ROC) curves [26], [27], [28], the area under ROC (AUC), and accuracy [29], [30] when the classification indexes of wake vortex cycle, background wind field and aircraft types are considered in this identification task.

Fig. 14 presents the ROC curves obtained from the different models tested in this experiment. It has been shown that ResNet mini v1 and ResNet mini v2 outperforms CNN, LeNet-5 and ShuffleNet v1 with respect to AUC, while they are close to SqueezeNet v1.

Table 2 summarizes the identification results on test set when the introduced models are applied to wake data when the classification indexes of wake vortex cycle, background wind field and aircraft types are included in identification task. The best results among all models are marked in bold. For the cycle stage 1, medium aircraft, heavy aircraft and overall accuracy, the best performances are achieved by ResNet mini v2. Although the accuracy of ResNet mini v1 for the indices of two cycle stages, background windspeed (around 4m/s) and light aircraft is slightly lower than its counterparts, the results obtained by the ResNet miniv1 is acceptable on classification indices background windspeed (around 1m/s), medium aircraft, heavy aircraft and overall accuracy.

It should be noted that ResNet mini v2 and ResNet mini v1 generate different performances on cycle stage 1 and cycle stage 2 respectively, which means that different models would learn different characteristics of the data.

For background wind field, the identification accuracy of these three models is much lower for stronger wind fields than that for weak wind fields. This means that the wind speed has a non-negligible effect on the wake vortex identification, and the higher the wind speed, the more difficult it is for the
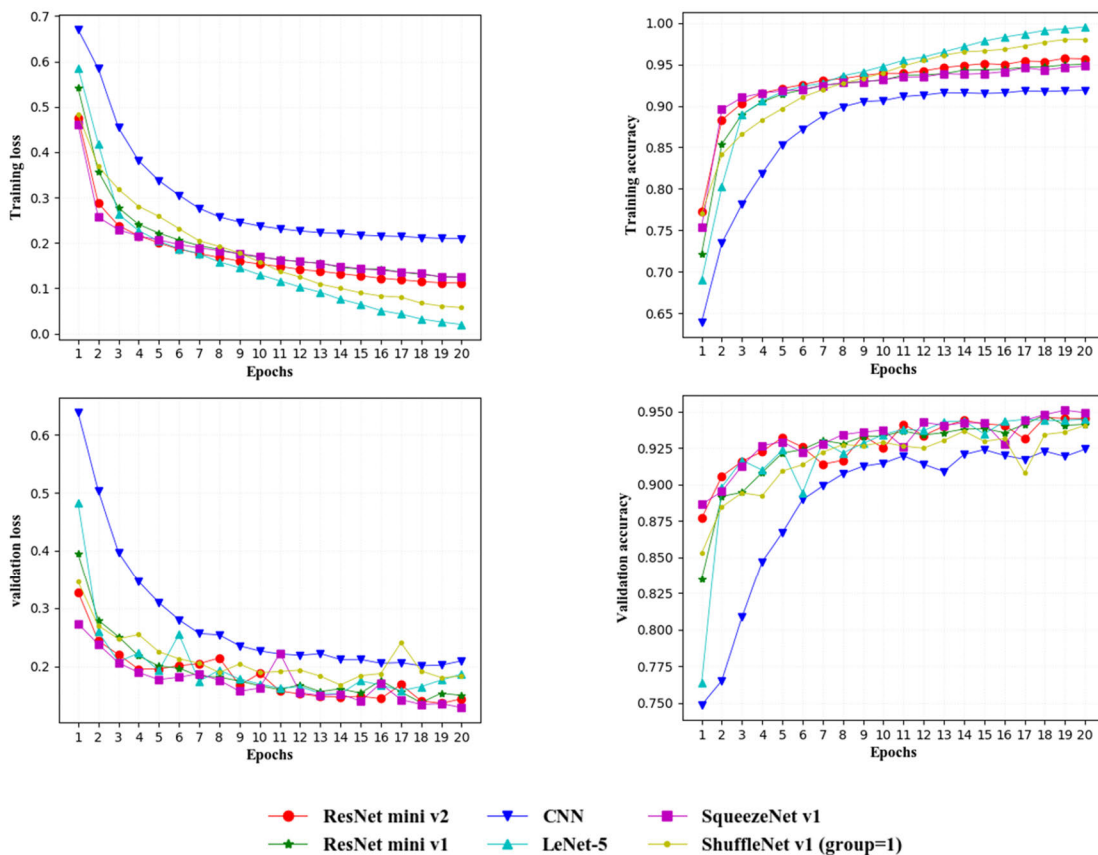
FIGURE 13. The loss and accuracy curves of models over epochs in training and validation for the wake vortex dataset.
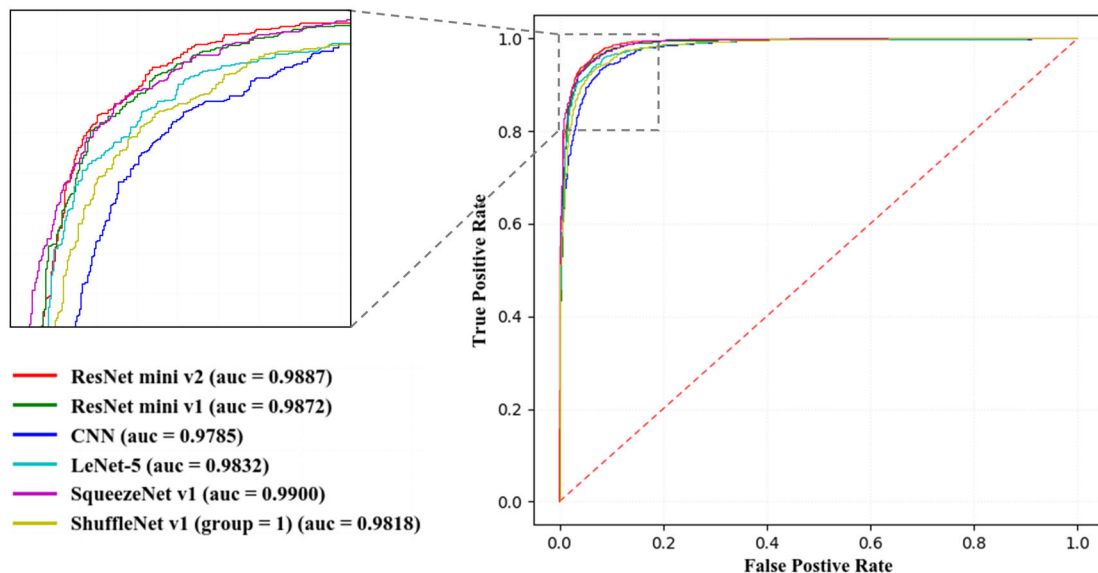
FIGURE 14. ROC plots of considered methods using the test set of our wake vortex dataset.

model to learn and identify its characteristics. In the actual airport environment, the average wind speed of the wind field usually changes greatly, and the different regions in airports often have more varied wind field environments due to the influence of meteorological, geographical and other factors. Therefore, the model's ability to identify wake vortex in
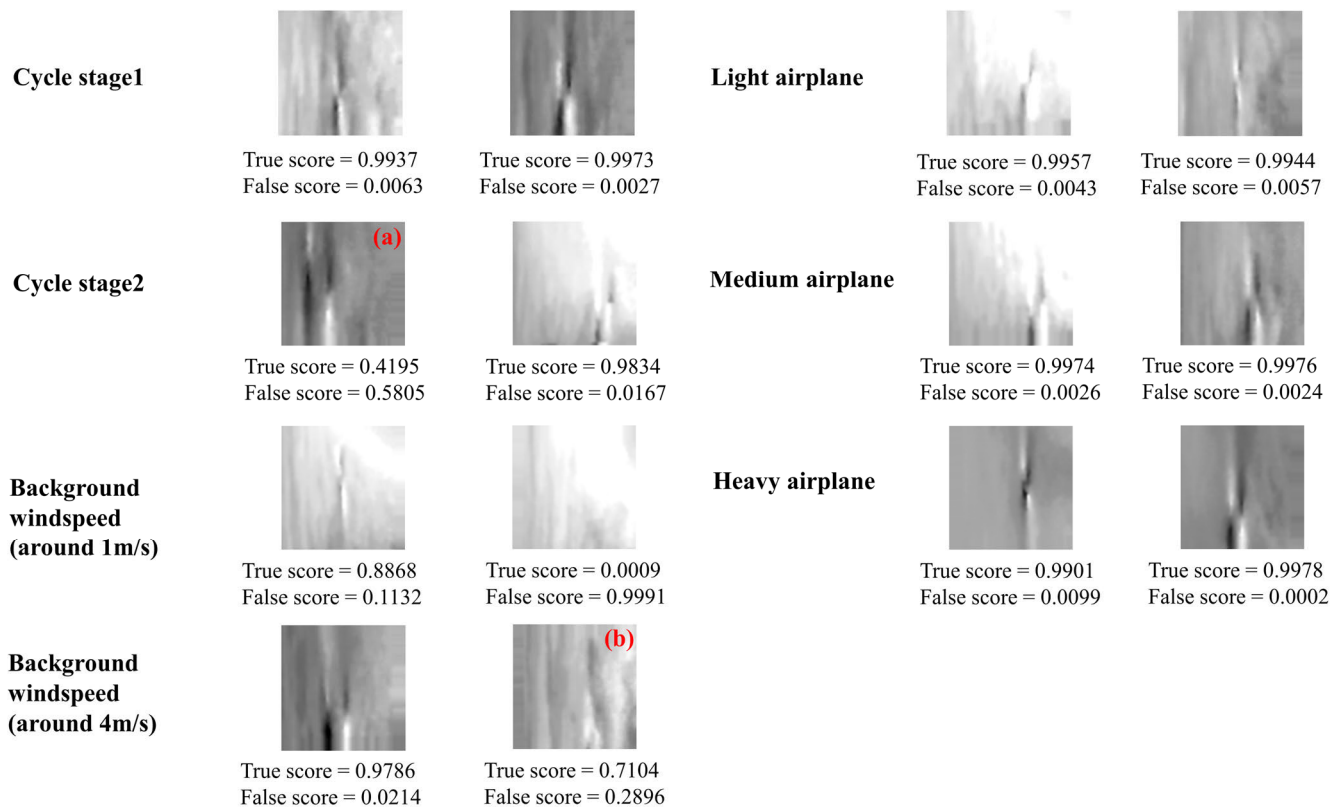
FIGURE 15. Part of experimental results obtained by ResNet mini v2. For the vast majority of wakes, it can be classified correctly. However, for some data with strong wind fields and more disordered, identification errors emergence. Subgraphs (a) and (b) are examples of identification failures.

strong wind fields is important for coping with more complex environments.

In the case of wake vortices from light aircraft, medium aircraft and heavy aircraft, the wake velocity and wake vortex volume decay gradually when the take-off weight decreases. Therefore, the accuracy of identifying the wake of heavy aircraft is greater than that of light aircraft or medium aircraft.

Fig. 15 is an example when ResNet mini v2 is applied on some wake vortices chosen from our test dataset. The performance of **Fig. 15** agrees with the results that have been shown in **Table 2**.

V. CONCLUSION

The exploration of information about aircraft wake vortex enables to obtain new knowledge of wake turbulence separation standards. Particularly, identifying the wake vortex in fine classification has great potential for practical application of the deep learning models in real airport environments. In our wake identification task, we grouped wake vortex into three classification indexes, namely, wake vortex cycle, background wind field and aircraft types. In addition, more efficient and lightweight networks that allow fewer parameters and calculations can meet the requirements of the users. Therefore, we developed two ResNet mini frameworks that are able to identify aircraft wake vortex with high accuracy in fine classification.

VI. LIMITATIONS & FUTURE WORK

1) The classification indexes are not likely to be sufficient to cover a wide range of wake vortex behaviors. We will make our approaches better in exploiting the features of wake vortices via mining effective pattern-based classification rules.

2) The designed scheme might affect the accuracy of the two proposed model. We will design a more efficient network to enhance the identification accuracy of wake vortices under effective pattern-based classification rules.

REFERENCES

[1] T. Gerz, F. Holzäpfel, and D. Daracq, "Commercial aircraft wake vortices," *Prog. Aerosp. Sci.*, vol. 38, no. 3, pp. 181–208, 2002.

[2] T. Misaka and S. Obayashi, "Numerical study on jet-wake vortex interaction of aircraft configuration," *Aerosp. Sci. Technol.*, vol. 70, pp. 615–625, Nov. 2017.

[3] J. Li, C. Shen, H. Gao, P. W. Chan, K. Hon, and X. Wang, "Path integration (PI) method for the parameter-retrieval of aircraft wake vortex by LiDAR," *Opt. Exp.*, vol. 28, no. 3, pp. 4286–4306, 2020.

[4] Z. Xu, D. Li, B. An, and W. Pan, "Enhancement of wake vortex decay by air blowing from the ground," *Aerosp. Sci. Technol.*, vol. 118, Nov. 2021, Art. no. 107029.

[5] S. Wu, X. Zhai, and B. Liu, "Aircraft wake vortex and turbulence measurement under near-ground effect using coherent Doppler LiDAR," *Opt. Exp.*, vol. 27, no. 2, pp. 1142–1163, 2019.

[6] F. Holzäpfel, "Sensitivity analysis of the effects of aircraft and environmental parameters on aircraft wake vortex trajectories and lifetimes," in *Proc. 51st AIAA Aerosp. Sci. Meeting Including New Horizons Forum Aerosp. Expo. (AIAA)*, Jan. 2013, p. 363.

[7] S. Kauertz, F. Holzäpfel, and J. Kladetzke, "Wake vortex encounter risk assessment for crosswind departures," *J. Aircr.*, vol. 49, no. 1, pp. 281–291, Jan. 2012.

[8] C. Shen, J. B. Li, F. L. Zhang, P. W. Chan, K. K. Hon, and X. S. Wang, "Two-step locating method for aircraft wake vortices based on Gabor filter and velocity range distribution," *IET Radar, Sonar Navigat.*, vol. 14, no. 12, pp. 1958–1967, 2020.

[9] J. Zhou, Y. Chen, D. Li, Z. Zhang, and W. Pan, "Numerical simulation of aircraft wake vortex evolution and wake encounters based on adaptive mesh method," *Eng. Appl. Comput. Fluid Mech.*, vol. 14, no. 1, pp. 1445–1457, Jan. 2020.

[10] W. Pan, Z. Wu, and X. Zhang, "Identification of aircraft wake vortex based on SVM," *Math. Problems Eng.*, vol. 2020, pp. 1–8, May 2020.

[11] J. N. Hallock and F. Holzäpfel, "A review of recent wake vortex research for increasing airport capacity," *Prog. Aerosp. Sci.*, vol. 98, pp. 27–36, Apr. 2018.

[12] W. Pan, H. Yin, Y. Leng, and X. Zhang, "Recognition of aircraft wake vortex based on random forest," *IEEE Access*, vol. 10, pp. 8916–8923, 2022.

[13] Y. Ai, Y. Wang, W. Pan, and D. Wu, "A deep learning framework based on multisensor fusion information to identify the airplane wake vortex," *J. Sensors*, vol. 2021, pp. 1–10, Nov. 2021.

[14] W. Pan, Y. Leng, H. Yin, and X. Zhang, "Identification of aircraft wake vortex based on VGGNet," *Wireless Commun. Mobile Comput.*, vol. 2022, pp. 1–10, Jun. 2022.

[15] W.-J. Pan, Y.-F. Leng, T.-Y. Wu, Y.-X. Xu, and X.-L. Zhang, "Conv-Wake: A lightweight framework for aircraft wake recognition," *J. Sensors*, vol. 2022, pp. 1–11, Jul. 2022.

[16] K. He, X. Zhang, S. Ren, and J. Sun, "Deep residual learning for image recognition," in *Proc. IEEE Conf. Comput. Vis. Pattern Recognit. (CVPR)*, Jun. 2016, pp. 770–778.

[17] Z. Wei, Z. Li, N. Zhuang, and R. Wen, "Evolution mechanism of aircraft wake vortex in ground proximity with the intervention of plate-line," [in Chinese] *J. Wuhan Univ. Sci. Technol.*, vol. 41, no. 02, pp. 153–160, Apr. 2018. [Online]. Available: https://kns.cnki.net/kcms2/article/abstract?v=3uoqIhG8C44YLTlOAiTRKibYlV5Vjs7i0-kJR0HYBJ80QN9L51zrP1YYUTABA3fpupabsPCaBANPdpkYJwQ8iwSC-tXBs6Vx&uniplatform=NZKPT

[18] A. Allen and C. Breitsamter, "Influence of a landing gear on the wake vortex evolution of a large transport aircraft," *AIAA J. Aircr.*, vol. 45, no. 3, p. 1367, 2008.

[19] X. Zhang, Z. Chen, Q. M. J. Wu, L. Cai, D. Lu, and X. Li, "Fast semantic segmentation for scene perception," *IEEE Trans. Ind. Informat.*, vol. 15, no. 2, pp. 1183–1192, Feb. 2019.

[20] S. Ioffe and C. Szegedy, "Batch normalization: Accelerating deep network training by reducing internal covariate shift," in *Proc. Int. Conf. Mach. Learn.*, 2015, pp. 448–456.

[21] G. Huang, Z. Liu, V. Laurens, and K. Q. Weinberger, "Densely connected convolutional networks," in *Proc. IEEE Conf. Comput. Vis. Pattern Recognit.* Washington, DC, USA: IEEE Computer Society, Jul. 2016, pp. 4700–4708.

[22] S. Ruder, "An overview of gradient descent optimization algorithms," 2016, *arXiv:1609.04747*.

[23] Y. LeCun, "LeNet-5, convolutional neural networks," *Lenet*, vol. 20, no. 5, p. 14, 2015. [Online]. Available: http://yann.lecun.com/exdb/lenet

[24] F. N. Iandola, S. Han, M. W. Moskewicz, K. Ashraf, W. J. Dally, and K. Keutzer, "SqueezeNet: AlexNet-level accuracy with 50x fewer parameters and <0.5 MB model size," 2016, *arXiv:1602.07360*.

[25] X. Zhang, X. Zhou, M. Lin, and J. Sun, "ShuffleNet: An extremely efficient convolutional neural network for mobile devices," in *Proc. IEEE/CVF Conf. Comput. Vis. Pattern Recognit.*, Jun. 2018, pp. 6848–6856.

[26] T. Fawcett, "An introduction to ROC analysis," *Pattern Recognit. Lett.*, vol. 27, no. 8, pp. 861–874, Jun. 2006.

[27] A. Saber, M. Sakr, O. M. Abo-Seida, A. Keshk, and H. Chen, "A novel deep-learning model for automatic detection and classification of breast cancer using the transfer-learning technique," *IEEE Access*, vol. 9, pp. 71194–71209, 2021.

[28] D. Luong, B. Balaji, and S. Rajan, "Performance prediction for coherent noise radars using the correlation coefficient," *IEEE Access*, vol. 10, pp. 8627–8633, 2022.

[29] X. Zhang, W. Pan, Z. Wu, J. Chen, Y. Mao, and R. Wu, "Robust image segmentation using fuzzy C-means clustering with spatial information based on total generalized variation," *IEEE Access*, vol. 8, pp. 95681–95697, 2020.

[30] S. Tural, R. Samet, S. Aydin, and M. Traore, "Deep learning based classification of military cartridge cases and defect segmentation," *IEEE Access*, vol. 10, pp. 74961–74976, 2022.

SIYUAN DUAN received the B.S. degree in traffic and transportation from the College of Air Traffic Management, Civil Aviation Flight University of China, Guanghan, China, in 2022.

He is currently a Research Assistant with the Tianfu Engineering-Oriented Numerical Simulation and Software Innovation Center, Sichuan University, Chengdu, China. His current research interests include deep learning, computer vision, and air traffic control automation.

WEIJUN PAN received the Ph.D. degree in computer application technology from Sichuan University, Chengdu, in 2013.

Since 1996, he has been with the Civil Aviation Flight University of China, Guanghan, China, where he is a Professor and the Dean with the College of Air Traffic Management. He is leading in the field of air traffic management, air traffic safety, and surveillance. He is the author of more than 50 papers. His research interests include aviation safety, air traffic management, and machine learning.

Dr. Pan acted as the Expert or Consultant to various academic organizations, such as the Chinese Society of Aeronautics and Astronautics. He hosted more than 30 research projects, such as the National Natural Science Foundation, the CAAC Research Foundation, the Sichuan Province Research Foundation, and international cooperation researches.
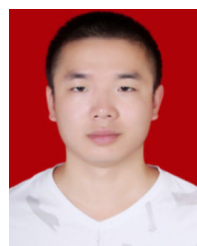
YUANFEI LENG received the B.S. degree in traffic and transportation engineering from the Chang'an University, Xi'an, in 2020. He is currently pursuing the M.S. degree in transportation with the Civil Aviation Flight University of China.

His research interests include artificial intelligence in air traffic management and aircraft wake interval reduction technology.

XIAOLEI ZHANG received the Ph.D. degree in control theory and control engineering from Nankai University, Tianjin, China, in 2014.

From 2015 to 2017, he was a Postdoctoral Research Fellow at Shantou University Medical College, Shantou, China. From 2017 to 2021, he was a Lecturer at the College of Air Traffic Management, Civil Aviation Flight University of China, Guanghan, China. He is currently with the Second Clinical Institute, Shantou University Medical College, Shantou, China, where he is a master's Supervisor. He is the author of more than 20 articles. His current research interests include deep learning, computer vision, and medical imaging.

• • •